Supplement of Atmos. Chem. Phys., 15, 9819–9849, 2015
http://www.atmos-chem-phys.net/15/9819/2015/
doi:10.5194/acp-15-9819-2015-supplement

Atmospheric Chemistry and Physics Open Access

Supplement of

Long-lived atmospheric trace gases measurements in flask samples from three stations in India

X. Lin et al.

Correspondence to: X. Lin (xin.lin@lsce.ipsl.fr)

Supplementary Materials

Table S1 Configurations and parameters of the GC system used in this study.

Code	CO_2/CH_4	N_2O/SF_6	CO/H_2
Carrier gas	N_2 5.0 50 mL min^{-1}	Ar/CH_4 40 mL min^{-1}	Synthetic air
Sample loop volume	15 mL	15 mL	1 mL
Over temperature	80 °C	80 °C	105 °C
Pre-column		Hayesep-Q 4'×3/16"OD, 80/100	Unibeads 1S 16.5"×1/8"OD, 60/80
Analytical column	Hayesep-Q 12'×3/16"OD, 80/100	Hayesep-Q 6'×3/16"OD, 80/100	Molecular Sieve 5Å 80"×1/8"OD, 60/80
Detector	FID: 250°C Ni catalyst: 390°C H_2: 100 mL min^{-1} Air : 300 mL min^{-1}	ECD: 395°C	RGD: 265°C
Calibration scale	CO_2: WMOX2007 CH_4: NOAA2004	N_2O: NOAA2005A SF_6: NOAA2005	CO: WMOX2004 H_2: WMOX2009

Table S2 Thresholds of differences between the pair of flask samples collected simultaneously for each trace gas species. Flask pairs exceeding the threshold are flagged and rejected.

Species	Threshold
CO_2	0.5 ppm
CH_4	5.0 ppb
N_2O	0.7 ppb
SF_6	0.5 ppt
CO	10.0 ppb
H_2	10.0 ppb

Table S3 Statistics of flask samples taken over the period 2007–2011. For each species at each station, the total number of flask sample pairs (N_{total}), the numbers of flask pairs retained ($N_{retained}$) and rejected ($N_{rejected}$) after flagging, and the number of flask pairs used to fit the smoothed curve (N_{fit}) are presented. The percentages of retained and rejected flask pairs, as well as the percentage of N_{fit} relative to $N_{retained}$, are also given in parentheses.

	N_{total}	N_{retain}	N_{rej}	N_{fit}
CO_2				
HLE	188	166 (88.3%)	22 (11.7%)	162 (97.6%)
PON	185	122 (65.9%)	63 (34.1%)	121 (99.2%)
PBL	63	45 (71.4%)	18 (28.6%)	44 (97.8%)
CH_4				
HLE	188	177 (94.1%)	11 (5.9%)	174 (98.3%)
PON	185	164 (88.6%)	21 (11.4%)	164 (100.0%)
PBL	63	57 (90.5%)	6 (9.5%)	56 (98.2%)
N_2O				
HLE	188	172 (91.5%)	16 (8.5%)	169 (98.3%)
PON	185	138 (74.6%)	47 (25.4%)	137 (99.3%)
PBL	63	55 (87.3%)	8 (12.7%)	55 (100.0%)
SF_6				
HLE	188	173 (92.0%)	15 (0.8%)	173 (100.0%)
PON	185	174 (94.1%)	11 (5.9%)	174 (100.0%)
PBL	63	61 (96.8%)	2 (3.2%)	61 (100.0%)
CO				
HLE	188	172 (91.5%)	16 (8.5%)	169 (98.3%)
PON	185	140 (75.7%)	45 (24.3%)	139 (99.3%)
PBL	63	55 (87.3%)	8 (12.7%)	53 (96.4%)
H_2				
HLE	188	163 (86.7%)	25 (13.3%)	160 (98.2%)
PON	185	141 (76.2%)	44 (23.8%)	140 (99.3%)
PBL	63	60 (95.2%)	3 (4.8%)	59 (98.3%)

Table S4 Uncertainties and bias of measured concentrations for each trace gas species.

Species	Analysis uncertainty	Sampling uncertainty	Bias
CO_2	0.07 ppm	0.42 ppm	-0.15±0.11 ppm
CH_4	0.73 ppb	1.34 ppb	0.09±1.70 ppb
N_2O	0.20 ppb	0.29 ppb	-0.11±0.88 ppb
SF_6	0.05 ppt	0 ppt	0.06±0.13 ppt
CO	0.81 ppb	2.50 ppb	3.5±2.2 ppb
H_2	1.32 ppb	2.39 ppb	-1.0±4.1 ppb

Table S5 Features of the smoothed fitting curves for flask measurements at PON (2007–2011). For each species, the smoothed curves are fitted to the data not filtered by CO outliers and the data filtered by CO outliers. The annual mean values and average peak-to-peak amplitude are calculated from the smoothed curve and mean season cycle, respectively. Uncertainty of each estimate is calculated from 1 s.d. of 1000 bootstrap replicates.

	Not CO filtered	CO filtered
CO_2 (ppm)		
N_{fit}	121	105
Annual mean 2007	386.6±0.9	386.5±1.1
Annual mean 2008	388.1±0.9	388.0±0.9
Annual mean 2009	389.0±0.6	388.4±0.8
Annual mean 2010	391.3±1.5	391.2±1.5
Annual gradient relative to HLE	2.9±1.2	2.6±1.4
Trend	1.7±0.1	1.7±0.1
RSD	4.0	4.1
Amplitude	7.6±1.4	7.8±1.6
D_{max}	111.0±13.4	116.0±14.1
D_{min}	327.0±54.3	327.0±55.8
CH_4 (ppb)		
N_{fit}	164	101
Annual mean 2007	1859.2±6.7	1854.2±5.9
Annual mean 2008	1856.1±10.4	1857.3±6.8
Annual mean 2009	1865.7±5.1	1855.5±6.2
Annual mean 2010	1876.9±9.1	1877.3±7.3
Annual gradient relative to HLE	37.4±10.7	34.0±11.0
Trend	9.4±0.1	9.0±0.1
RSD	34.4	19.8
Amplitude	124.1±10.2	127.8±11.4
D_{max}	337.0±6.1	331.0±5.4
D_{min}	189.0±10.7	192.0±9.8
N_2O (ppb)		
N_{fit}	137	110
Annual mean 2007	324.8±0.3	324.9±0.4
Annual mean 2008	326.3±0.3	326.3±0.3
Annual mean 2009	326.7±0.3	326.4±0.3
Annual mean 2010	327.1±0.5	327.0±0.5
Annual gradient relative to HLE	3.1±0.3	3.0±0.3
Trend	0.8±0.1	0.7±0.1
RSD	1.4	1.4
Amplitude	1.2±0.5	1.1±0.5
D_{max}	262.0±83.2	262.0±46.1

D_{min}	141.0±48.2	97.0±65.8
SF_6 (ppt)		
N_{fit}	174	139
Annual mean 2007	6.19±0.01	6.19±0.02
Annual mean 2008	6.49±0.02	6.49±0.02
Annual mean 2009	6.77±0.01	6.77±0.02
Annual mean 2010	7.08±0.02	7.08±0.02
Annual gradient relative to HLE	-0.06±0.03	-0.06±0.03
Trend	0.31±0.05	0.31±0.06
RSD	0.05	0.05
Amplitude	0.24±0.02	0.24±0.03
D_{max}	327.0±12.1	327.0±21.7
D_{min}	204.0±3.3	205.0±3.4
CO (ppb)		
N_{fit}	139	139
Annual mean 2007	200.5±7.8	200.5±7.8
Annual mean 2008	175.3±13.1	175.3±13.1
Annual mean 2009	174.3±4.8	174.3±4.8
Annual mean 2010	185.1±8.7	185.1±8.7
Annual gradient relative to HLE	82.4±10.7	82.4±10.7
Trend	0.4±0.1	0.4±0.1
RSD	32.0	32.0
Amplitude	78.2±11.6	78.2±11.6
D_{max}	4.0±160.2	4.0±160.2
D_{min}	238.0±46.1	238.0±46.1
H_2 (ppb)		
N_{fit}	140	120
Annual mean 2007	574.5±2.4	573.7±3.2
Annual mean 2008	558.2±5.3	558.3±5.1
Annual mean 2009	562.4±1.6	561.9±1.6
Annual mean 2010	563.9±2.3	563.0±2.5
Annual gradient relative to HLE	29.8±4.1	29.3±3.7
Trend	-1.3±0.1	-1.3±0.1
RSD	8.4	8.3
Amplitude	21.6±3.4	21.1±3.8
D_{max}	96.0±9.6	97.0±9.8
D_{min}	219.0±10.3	215.0±11.9

Table S6 List of atmospheric ground stations, of which flask and/or in-situ measurements were analyzed in this study.

Code	Station	Latitude (°)	Longitude (°)	Altitude (m a.s.l.)	Contributor(s)
BGU	Begur, Spain	41.97 °N	3.3 °E	30.00	ICOS, Laboratoire des Sciences du Climat et de l'Environnement
BKT	Bukit Kototabang, Indonesia	0.20 °S	100.32 °E	845.00	NOAA/ESRL, Bureau of Meteorology and Geophysics, The Swiss Federal Laboratories for Materials Science and Technology
BMW	Tudor Hill, Bermuda, United Kingdom	32.26 °N	64.88 °W	30.00	NOAA/ESRL, Bermuda Institute of Ocean Sciences
FIK	Finokalia, Greece	35.34 °N	25.67 °E	152.00	ICOS, Laboratoire des Sciences du Climat et de l'Environnement
GMI	Mariana Islands, Guam	13.39 °N	144.66 °E	0.00	NOAA/ESRL, University of Guam/Marine Laboratory
HLE	Hanle, India	32.78 °N	78.96 °E	4517.00	Indo-French Network, Laboratoire des Sciences du Climat et de l'Environnement, Indian Institute of Astrophysics
HFM	Harvard Forest, Massachusetts, United States	42.54 °N	72.17 °W	340.00	NOAA/ESRL
KZM	Plateau Assy, Kazakhstan	43.25 °N	77.88 °E	2519.00	NOAA/ESRL, Kazakh Scientific Institute of Environmental Monitoring and Climate
LEF	Park Falls, Wisconsin, United States	45.95 °N	90.27 °W	472.00	NOAA/ESRL, Wisconsin Educational Communications Board & US Forest Service, MBMAS, USDA Forest Service Forestry Sciences Laboratory, USDA Forest Service
LPO	Ile Grande, France	48.80 °N	3.57 °W	30.00	ICOS, Laboratoire des Sciences du Climat et de l'Environnement
MHD	Mace Head, Ireland	53.33 °N	9.90 °W	25.00	ICOS, Laboratoire des Sciences du Climat et de l'Environnement
MID	Sand Island, Midway, United States	28.21 °N	177.38 °W	11.00	NOAA/ESRL, U.S. Fish and Wildlife Service
MLO	Mauna Loa, Hawaii, United States	19.54 °N	155.58 °W	3397.00	NOAA/ESRL
NWR	Niwot Ridge, Colorado, United States	40.05 °N	105.59 °W	3523.00	NOAA/ESRL, University of Colorado/INSTAAR
PBL	Port Blair, India	11.55 °N	92.73 °E	20.00	Indo-French Network, Laboratoire des Sciences du Climat et de l'Environnement, National Institute of Ocean Technology, India
PON	Pondicherry, India	12.01 °N	79.86 °E	20.00	Indo-French Network, Laboratoire des Sciences du Climat et de l'Environnement, Pondicherry University, CSIR Fourth Paradigm Institute, India
WIS	Negev Desert, Israel	30.86 °N	34.78 °E	477.00	NOAA/ESRL, Weizmann Institute of Science
WLG	Mt. Waliguan, China	36.29 °N	100.90 °E	3810.00	NOAA/ESRL, Chinese Academy of Meteorological Sciences, Qinghai Meteorological Bureau, China Meteorological Administration

Table S7 Annual mean values, trends, and average peak-to-peak amplitudes of N_2O at MHD, BGU, FIK, LPO, NWR, HFM and LEF. For each species at each station, the annual mean values and average peak-to-peak amplitude are calculated from the smoothed curve and mean seasonal cycle, respectively. The residual standard deviation (RSD) around the smoothed curve and the Julian days corresponding to the maximum (D_{max}) and minimum (D_{min}) of the mean seasonal cycle are given as well. Uncertainty of each estimate is calculated from 1 SD of 1000 bootstrap replicates. Here MHD, BGU, FIK and LPO belong to the ICOS network, whereas NWR, HFM and LEF belong to the NOAA/ESRL network (Table S6, Figure S1). The grey shaded columns indicate results for the reference stations.

	MHD	**BGU**	**FIK**	**LPO**	**NWR**	**HFM**	**LEF**
N_2O (ppb)							
Annual mean 2007	321.9±0.1	323.0±0.1	322.5±0.1	324.3±0.2	320.6±0.1	321.3±0.1	321.1±0.1
Annual mean 2008	322.6±0.1	323.8±0.1	323.1±0.1	325.3±0.3	321.5±0.1	322.0±0.1	321.7±0.1
Annual mean 2009	323.2±0.1	324.4±0.1	323.5±0.1	325.5±0.2	322.7±0.1	323.2±0.0	323.0±0.1
Annual mean 2010	324.2±0.1	325.5±0.1	324.4±0.1	325.5±0.2	323.5±0.1	324.0±0.1	323.8±0.1
Annual mean 2011	325.0±0.1	325.8±0.1	325.5±0.1	326.6±0.3	324.7±0.1	325.2±0.1	325.0±0.1
Trend	0.8±0.1	0.5±0.0	0.7±0.1	0.7±0.0	1.0±0.0	0.9±0.0	1.0±0.0
RSD	0.3	0.6	0.2	0.9	0.3	0.5	0.6
Amplitude	1.0±0.1	1.3±0.4	0.2±0.1	1.3±0.3	0.2±0.1	0.5±0.1	0.5±0.1
D_{max}	102.0±64.3	303.0±15.8	144.0±80.3	138.0±57.1	259.0±85.4	350.0±148.0	77.0±79.6
D_{min}	229.0±5.6	186.0±32.7	253.0±76.4	39.0±79.5	354.0±122.1	227.0±28.0	215.0±25.7

Table S8 Student's t-test statistics for significance of N_2O seasonal differences. The original flask data are detrended and divided into Group X and Y according to the seasonal maximum/minimum identified by the smoothed curve fitting procedure. For each group X and Y, Student's t-test is performed to give the t-test statistics.

Site	Description of Group X and Y	X mean	Y mean	t statistic	df	p value
HLE	X: flask data in Aug. (seasonal maximum) Y: flask data in other months Alternative hypothesis: X > Y	0.28	-0.08	1.78	8.36	0.06
HLE	X: flask data in Feb. (secondary maximum) Y: flask data in Nov.–Jan. and Mar.–May Alternative hypothesis: X > Y	-0.20	-0.11	-0.84	16.36	0.79
PON	X: flask data in Aug.–Nov. (seasonal maximum) Y: flask data in other months Alternative hypothesis: X > Y	0.48	-0.06	1.54	77.15	0.06
PON	X: flask data in Apr.–Jun. (seasonal minimum) Y: flask data in other months Alternative hypothesis: X < Y	-0.31	0.25	-1.46	49.50	0.07
PBL	X: flask data in Oct.–Dec. (seasonal maximum) Y: flask data in other months Alternative hypothesis: X > Y	0.40	-0.23	1.76	42.08	0.04

Table S9 Annual mean values, trends, and average peak-to-peak amplitudes of SF_6 at MLO, MHD, BGU, LPO, NWR and HFM. For each species at each station, the annual mean values and average peak-to-peak amplitude are calculated from the smoothed curve and mean seasonal cycle, respectively. The residual standard deviation (RSD) around the smoothed curve and the Julian days corresponding to the maximum (D_{max}) and minimum (D_{min}) of the mean seasonal cycle are given as well. Uncertainty of each estimate is calculated from 1 SD of 1000 bootstrap replicates. Here MHD, BGU and LPO belong to the ICOS network, whereas NWR and HFM belong to the NOAA/ESRL network (Table S6, Figure S1). The grey shaded columns indicate results for the reference stations.

	MLO	**MHD**	**BGU**	**LPO**	**NWR**	**HFM**
SF_6 (ppt)						
Annual mean 2007	6.27±0.01	6.31±0.01	6.43±0.02	6.39±0.04	6.30±0.01	6.55±0.05
Annual mean 2008	6.55±0.01	6.61±0.01	6.74±0.03	6.65±0.02	6.62±0.01	6.78±0.02
Annual mean 2009	6.85±0.01	6.92±0.01	7.02±0.03	6.96±0.02	6.87±0.01	7.00±0.01
Annual mean 2010	7.14±0.01	7.18±0.01	7.27±0.02	7.21±0.01	7.18±0.01	7.32±0.03
Annual mean 2011	7.41±0.01	7.49±0.01	7.56±0.03	7.52±0.02	7.49±0.01	7.58±0.02
Trend	0.29±0.03	0.29±0.05	0.28±0.04	0.28±0.05	0.29±0.04	0.22±0.04
RSD	0.04	0.04	0.14	0.11	0.04	0.33
Amplitude	0.04±0.01	0.07±0.01	0.07±0.03	0.10±0.03	0.02±0.01	0.15±0.07
D_{max}	297.0±65.4	26.0±38.2	95.0±109.9	344.0±132.7	96.0±36.2	340.0±116.8
D_{min}	32.0±81.3	264.0±11.1	201.0±47.8	229.0±213.2	1.0±116.0	81.0±51.1

Table S10 Student's t-test statistics for significance of SF_6 seasonal differences. The original flask data are detrended and divided into Group X and Y according to the seasonal maximum/minimum identified by the smoothed curve fitting procedure. For each group X and Y, Student's t-test is performed to give the t-test statistics.

Site	Description of Group X and Y	X mean	Y mean	t statistic	df	p value
HLE	X: flask data in Nov. (seasonal maximum) Y: flask data in other months Alternative hypothesis: X > Y	0.098	0.001	2.425	15.242	0.014
HLE	X: flask data in May. (secondary maximum) Y: flask data in Feb.–Apr. and Jun.–Aug. Alternative hypothesis: X > Y	0.0003	-0.035	2.443	21.412	0.016
HLE	X: flask data in Aug.–Nov. (seasonal minimum) Y: flask data in other months Alternative hypothesis: X < Y	0.0003	0.019	-1.153	33.793	0.128
PON	X: flask data in Nov.–Dec. (seasonal maximum) Y: flask data in other months Alternative hypothesis: X > Y	0.081	-0.018	5.621	43.153	<0.001
PBL	X: flask data in Nov.–Dec. (seasonal maximum) Y: flask data in other months Alternative hypothesis: X > Y	0.278	-0.071	5.138	20.334	<0.001

Table S11 Annual mean values, trends, and average peak-to-peak amplitudes of H_2 at HLE and PON, in comparison to NOAA/ESRL stations at similar latitudes – BMW, MID and GMI. For each species at each station, the annual mean values and average peak-to-peak amplitude are calculated from the smoothed curve and mean seasonal cycle, respectively. The residual standard deviation (RSD) around the smoothed curve and the Julian days corresponding to the maximum (D_{max}) and minimum (D_{min}) of the mean seasonal cycle are given as well. Uncertainty of each estimate is calculated from 1 SD of 1000 bootstrap replicates. The grey shaded columns indicate results for the reference stations.

	HLE	**BMW**	**MID**	**PON**	**GMI**
H_2 (ppb)					
Annual mean 2004	–	524.0±1.4	523.6±1.4	–	538.1±1.2
Annual mean 2005	–	523.0±1.7	525.9±1.5	–	540.9±0.7
Annual mean 2006	–	518.3±1.2	520.5±0.7	–	532.6±0.5
Annual mean 2007	539.6±2.1	515.0±1.6	521.6±1.1	574.5±2.4	535.7±0.8[a]
Annual mean 2008	533.2±3.2	–	–	558.2±5.3	–
Annual mean 2009	533.3±1.6	–	–	562.4±1.6	–
Annual mean 2010	533.5±1.8	–	–	563.9±2.3	–
Annual mean 2011	536.9±1.5	–	–	–	–
Trend	-0.5±0.0	-3.2±0.1	-0.8±0.1	-1.3±0.1	-1.1±0.1
RSD	6.6	6.4	6.9	8.4	4.4
Amplitude	15.8±2.2	39.6±2.6	38.0±2.4	21.6±3.4	21.5±1.2
D_{max}	120.0±8.7	196.0±4.9	183.0±3.5	96.0±9.6	146.0±7.7
D_{min}	266.0±39.6	325.0±4.9	316.0±5.6	219.0±10.3	362.0±163.2

[a] This value is averaged over the smoothed curve segment from Jan. 1st to Nov. 23rd 2007.

Table S12 The $\Delta CH_4/\Delta CO$ ratios documented in previous studies, indicating urban/industrial sources. Underlined ratios in the table indicate the cases influenced by winter air masses from the Siberian region with substantial oil and natural gas extraction.

No.	Reference	Campaign	Sampling type	Sampling region (location)	Sampling height	Sampling period	$\Delta CH_4/\Delta CO$ (ppb/ppb)
1	Harriss et al., 1994	ABLE 3B	Aircraft, in-situ	Eastern Canada	0.15–6 km	Jul.–Aug. 1990	0.84
2	Bakwin et al., 1995		Ground station, flask	Eastern North Carolina (35.37 °N, 77.39 °W, 9 m a.s.l.)	496 m	Jun. 1992–Jun. 1994	0.76±0.10
3	Harris et al., 2000		Ground station, in-situ	Barrow, Alaska (BRW – 71.32 °N, 156.62°W, 9 m a.s.l.)		Nov.–Jan. 1986–1997	1.69±0.11
4	Sawa et al., 2004	PACE-7	Aircraft, flask	Western North Pacific	5 km	Feb. 2000	0.4
5	Sawa et al., 2004	PACE-7	Aircraft, flask	Western North Pacific	8–11 km	Feb. 2000	1.2
6	Xiao et al., 2004	TRACE-P	Aircraft, in-situ	NW Pacific: Chinese outflow (>30°N)	0–2 km	Mar.–Apr. 2001	0.38±0.02
7	Xiao et al., 2004	TRACE-P	Aircraft, in-situ	NW Pacific: Tropical Asian outflow (20–30°N)	0–2 km	Mar.–Apr. 2001	0.46±0.02
8	Xiao et al., 2004	TRACE-P	Aircraft, in-situ	NW Pacific: Japanese/Korean Outflow		Mar.–Apr. 2001	0.65±0.03
9	Xiao et al., 2004	TRACE-P	Aircraft, in-situ	NW Pacific: Background (East of 160 °E)	2–8 km	Mar.–Apr. 2001	0.75±0.04
10	Lai et al., 2010	CARIBIC	Aircraft, in-situ	South China to Philippines	9–11 km	Apr. 2007	0.3–0.8
11	Wada et al., 2011		Ground station, in-situ	Minamitorishima (MNM – 24.28 °N, 153.98 °E, 8.00 m a.s.l.)	10 m	2008	0.5–1.6
12	Wada et al., 2011		Ground station, in-situ	Yonagunijima (YON – 24.47 °N, 123.02 °E, 30.00 m a.s.l.)	10 m	2008	0.3–1.0
13	Wada et al., 2011		Ground station, in-situ	Ryori (RYO – 39.03 °N, 141.82 °E, 260 m a.s.l.)	10 m	2008	0.3–0.6
14	Chi et al., 2013		Ground station, in-situ	Zotino (60.80 °N, 89.35°E, 114 m a.s.l.)	300 m	Winter, 2006-2011	1.21–1.30
15	Niwa et al., 2014		Aircraft, flask	Western North Pacific	~6 km	Dec.–Mar. 2010–2012	0.47
16	Niwa et al., 2014		Aircraft, flask	Western North Pacific	~6 km	Jul.–Oct. 2010–2012	1.2

Abbreviations: ABLE 3B – Arctic Boundary Layer Expeditions 3B; CARIBIC – Civil Aircraft for the Regular Investigation of the atmosphere Based on an Instrumented Container; PACE-7 – Pacific Atmospheric Chemistry Experiment 7; TRACE-P – Transport and Chemical Evolution over the Pacific

Figure S1 Map of locations of atmospheric ground stations corresponding to Table S6. The background is plotted based on SRTM 1 km Digital Elevation Data (http://srtm.csi.cgiar.org). Locations of stations are colored according to the network they belong to (blue: ICOS; red: NOAA/ESRL; purple: Indo-French Network).

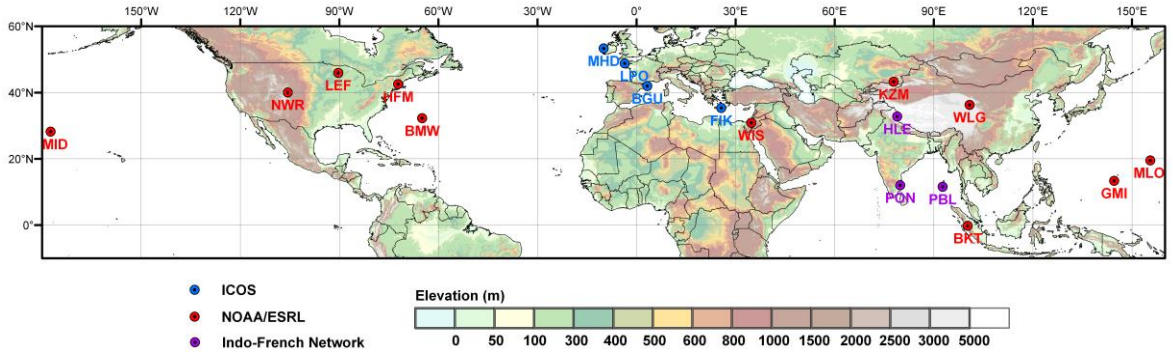

Figure S2 Time series of flask measurements at PON (2007–2011) with smoothed fitting curves for **(a)** CO_2, **(b)** CH_4, **(c)** N_2O, **(d)** SF_6 and **(e)** H_2. The open circles denote flask data used to fit the solid smoothed curves, while the crosses denote discarded flask data lying outside 3 times the residual standard deviations from the smoothed curve fits as well as those filtered by CO outliers. For PON, the solid (dotted) red line indicates the smoothed curve fitted to the data (not) filtered by CO outliers. The flask measurements at HLE and the corresponding smoothed fitting curve are also presented for comparison.

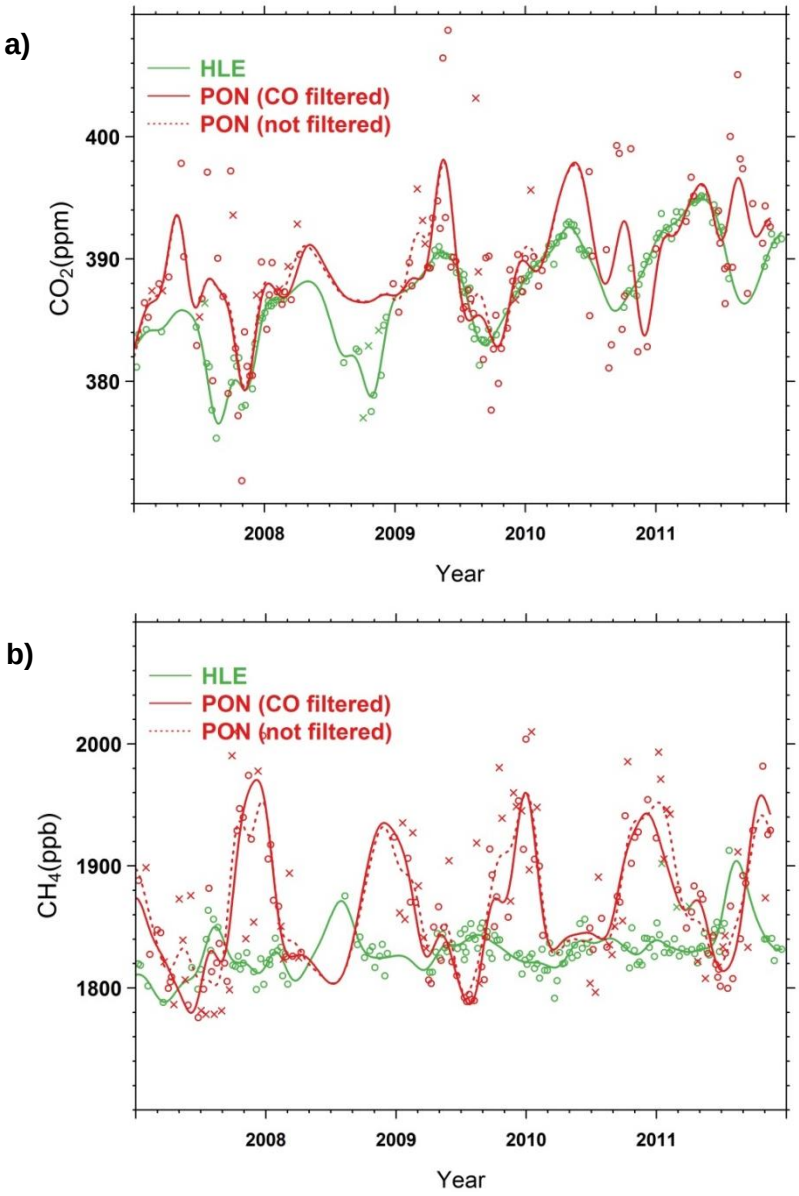

78

79

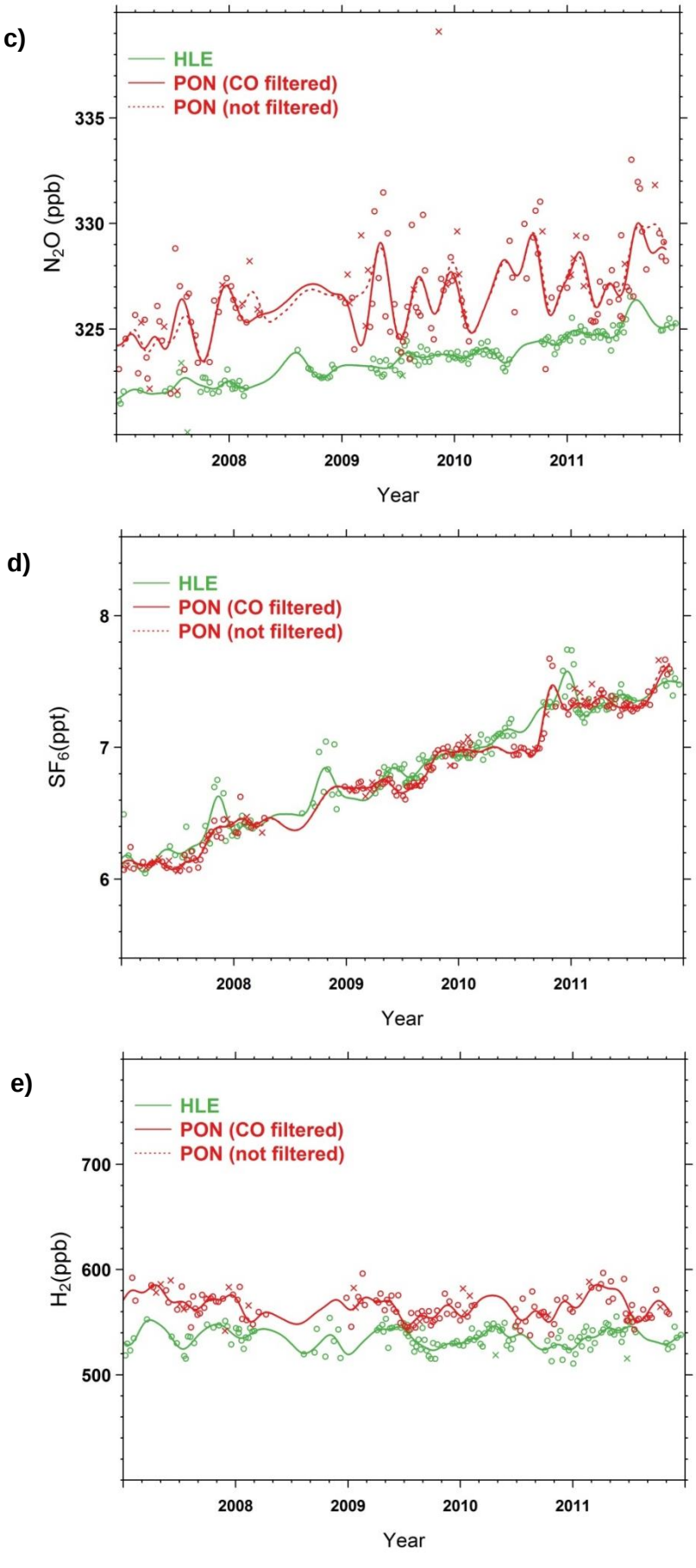
c)
HLE
PON (CO filtered)
PON (not filtered)
335
330
325
N2O (ppb)
2008
2009
2010
2011
Year
d)
HLE
PON (CO filtered)
PON (not filtered)
8
7
6
SF6(ppt)
2008
2009
2010
2011
Year
e)
HLE
PON (CO filtered)
PON (not filtered)
700
600
500
H2(ppb)
2008
2009
2010
2011
Year

Figure S3 Flask sampling dates of atmospheric ground stations that are used to fit the smoothed curves in this study. Locations of stations are presented in Table S6 and Figure S1.

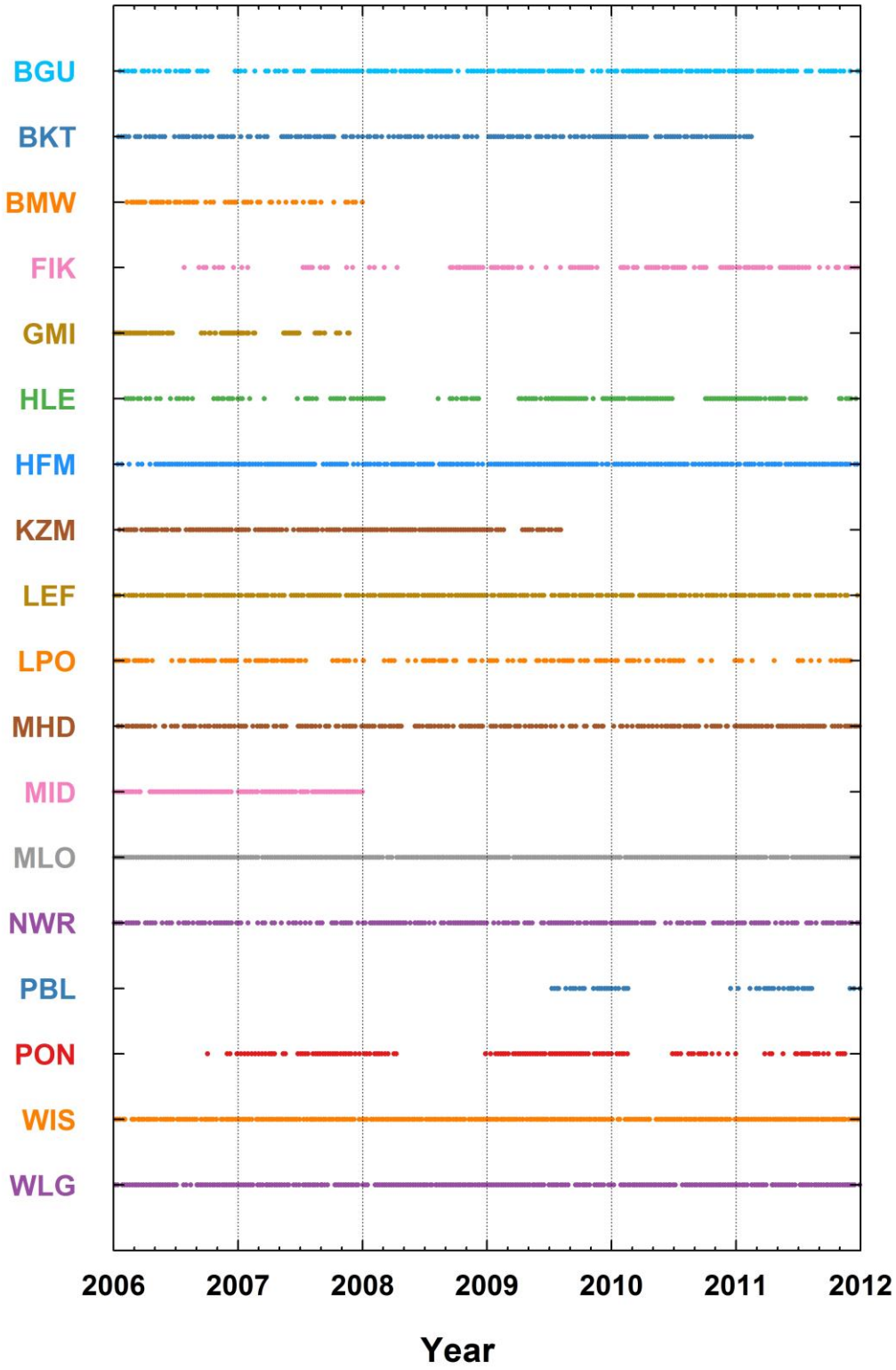

Figure S4 The mean CO_2 seasonal cycles at **a)** HLE, **b)** KZM, and **c)** WLG, in comparison to the composite zonal marine boundary layer (MBL) references at 32°N–33°N, 43°N–44°N, and 36°N–37°N, respectively. Shaded area indicates the uncertainty of the mean seasonal cycle calculated from 1 SD of 1000 bootstrap replicates.

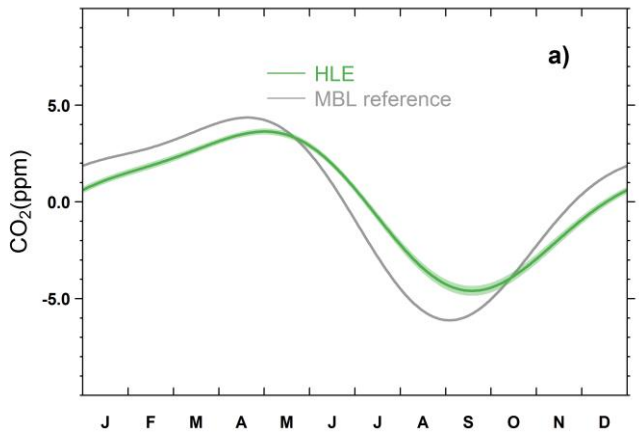

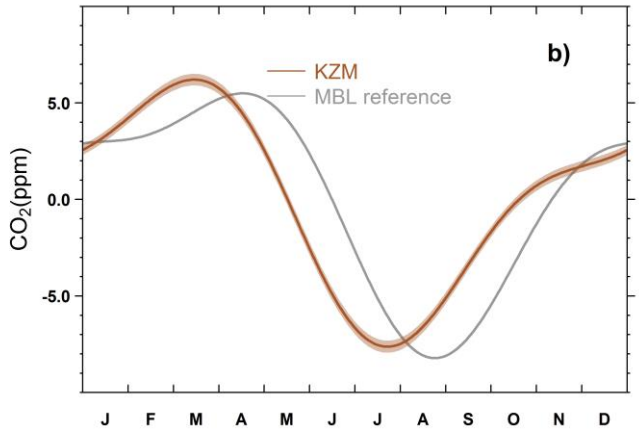

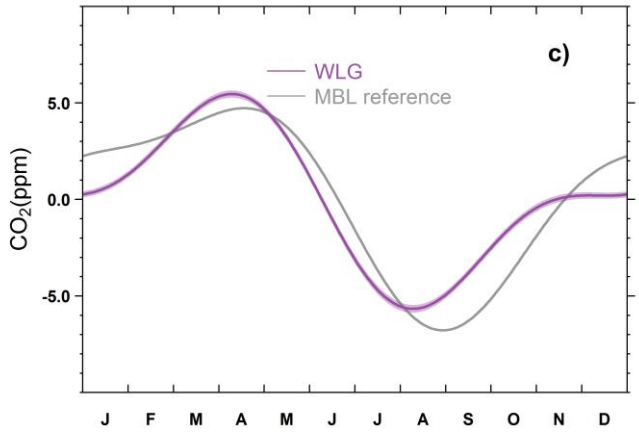

Figure S5 Five-day back trajectories calculated for all sampling dates over the period 2007–2011 at **a)** KZM and **b)** WLG during April–June (AMJ), July–September (JAS), October–December (OND) and January–March (JFM), respectively. All back-trajectories are colored by the elevation of air masses at hourly time step.

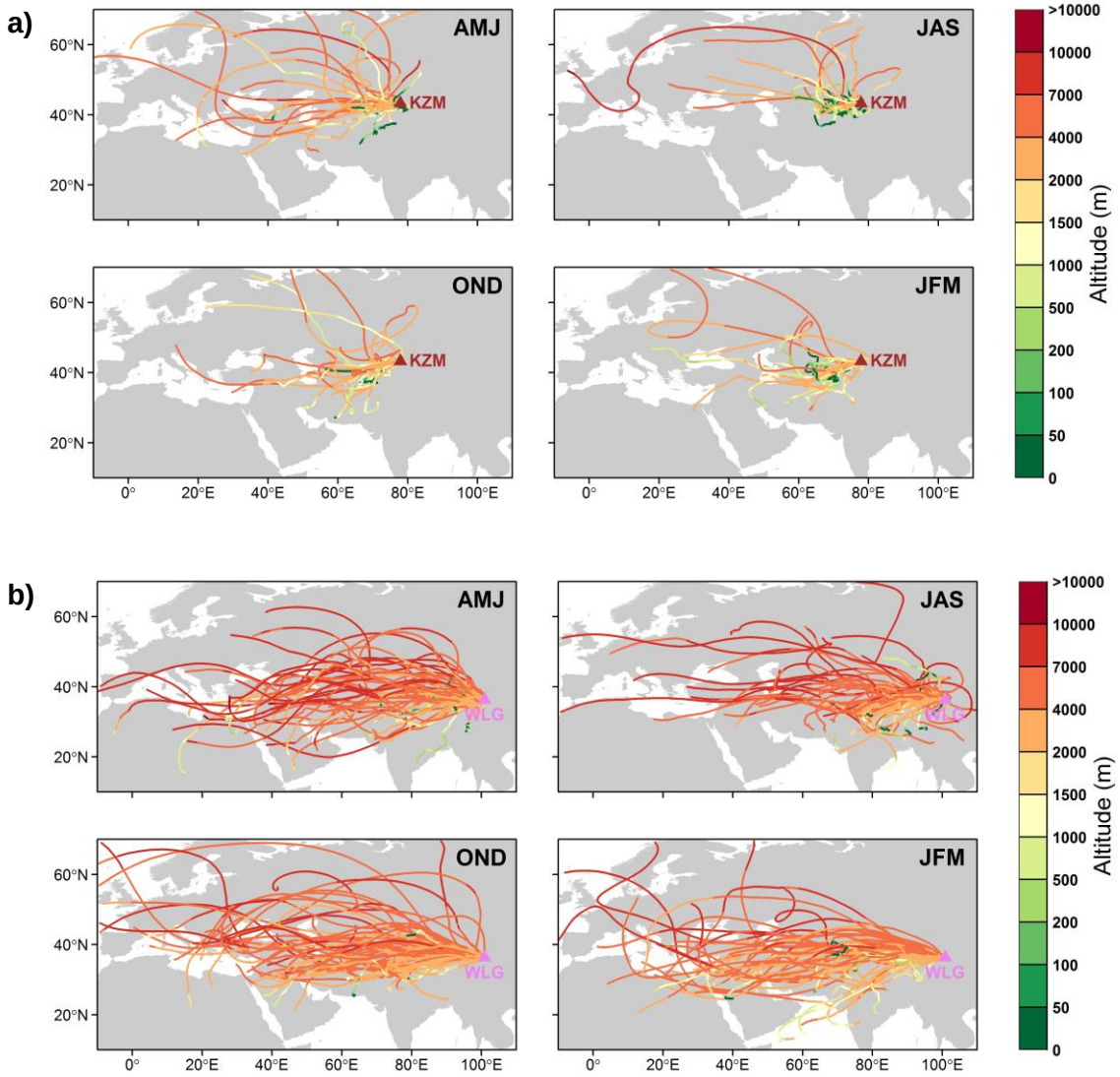

Figure S6 Vertical cross-sections of five-day back trajectories calculated for all sampling dates over the period of 2007–2011 at **a)** HLE, **b)** PON, **c)** PBL, **d)** KZM, and **e)** WLG during April–June (AMJ), July–September (JAS), October–December (OND), and January–March (JFM), respectively. Back trajectories are colored according to individual CO_2 measurements on the corresponding sampling dates.

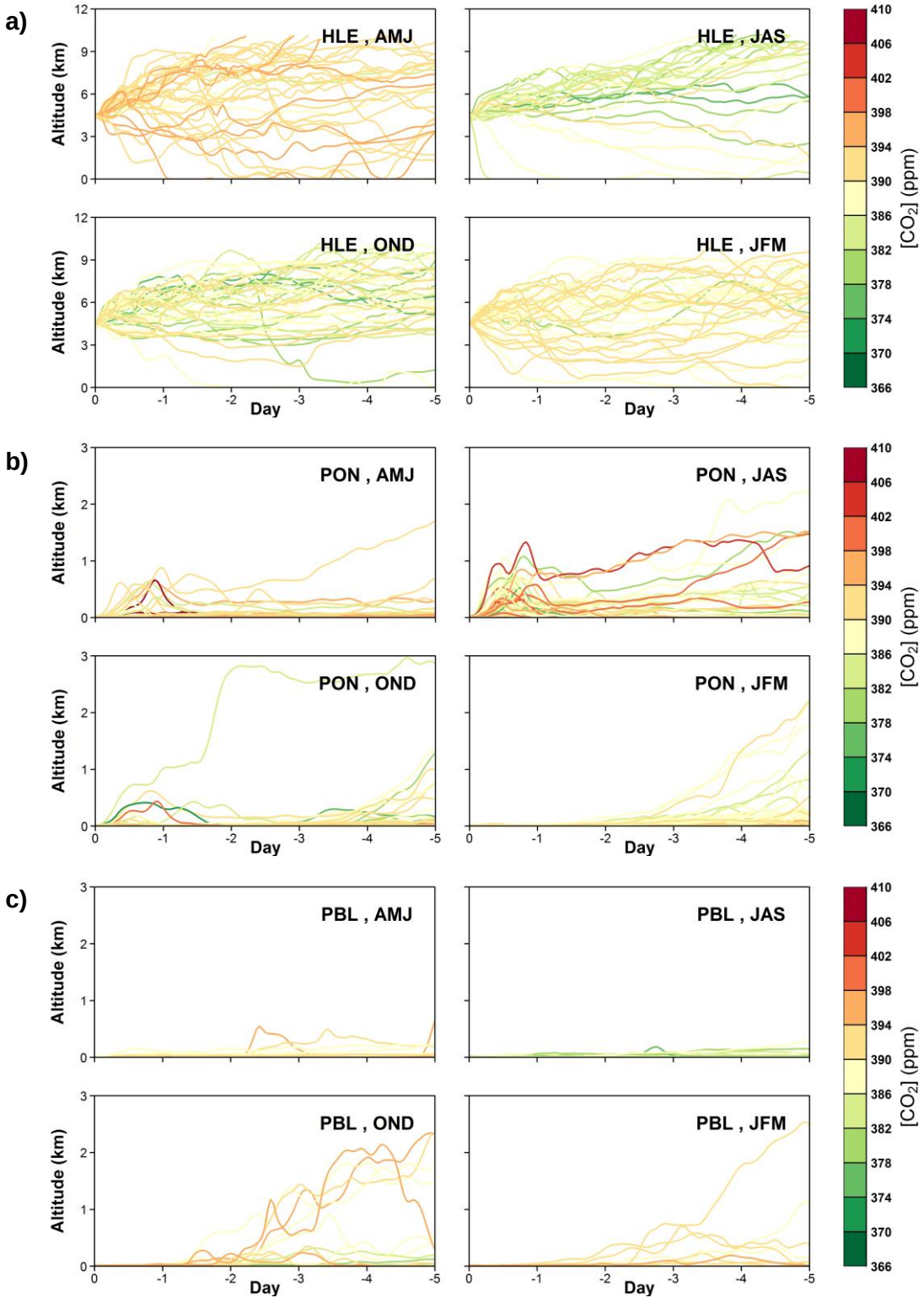

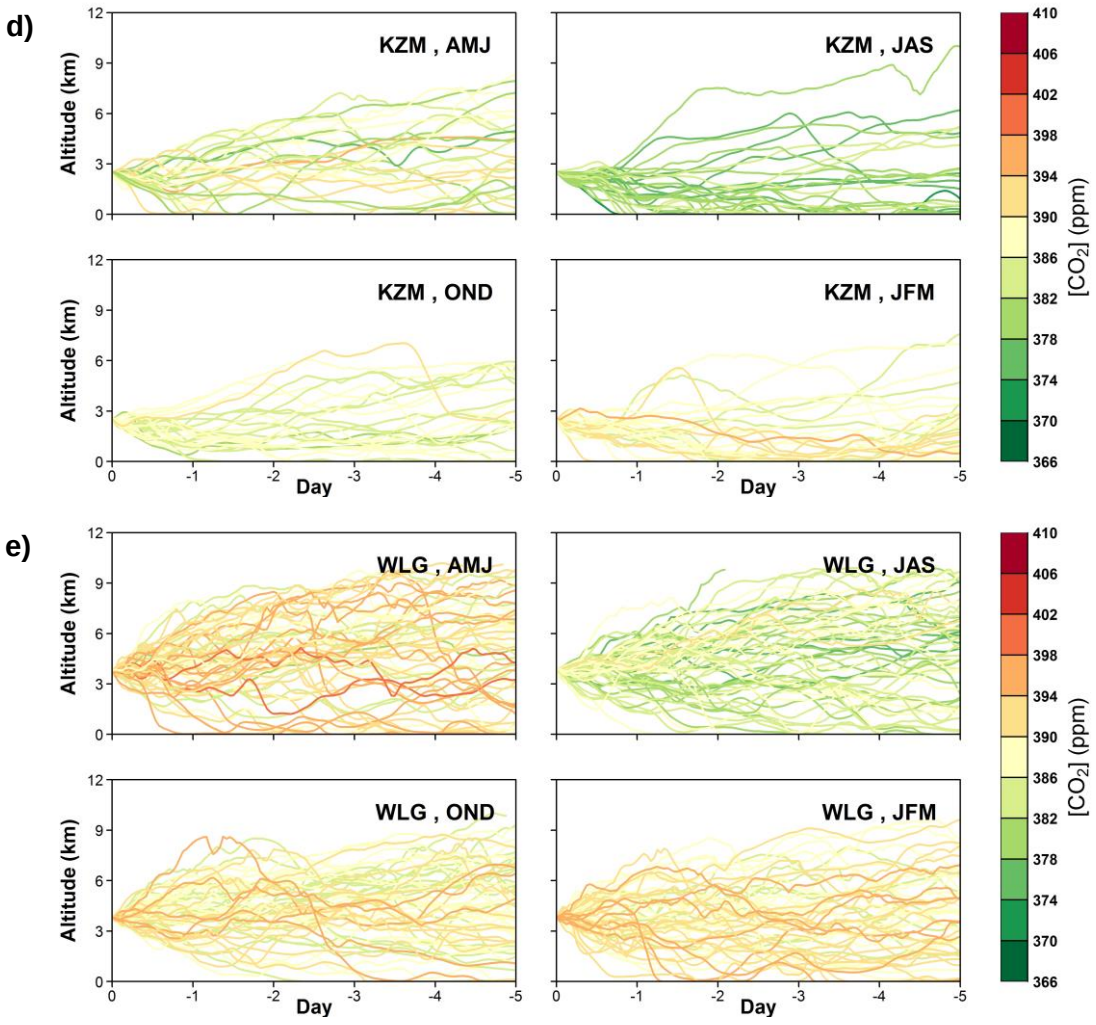
d)
KZM , AMJ
KZM , JAS
KZM , OND
KZM , JFM
Altitude (km)
Day
e)
WLG , AMJ
WLG , JAS
WLG , OND
WLG , JFM
[CO2] (ppm)

Figure S7 Five-day back trajectories calculated for all sampling dates over the period 2007–2011 at Hanle (HLE), Pondicherry (PON), and Port Blair (PBL) during April–June (AMJ), July–September (JAS), October–December (OND) and January–March (JFM), respectively. Back trajectories are colored according to flask measurements of **a)** CO_2, **b)** CH_4, **c)** N_2O, **d)** SF_6, **e)** CO, and **f)** H_2 on the corresponding sampling dates.

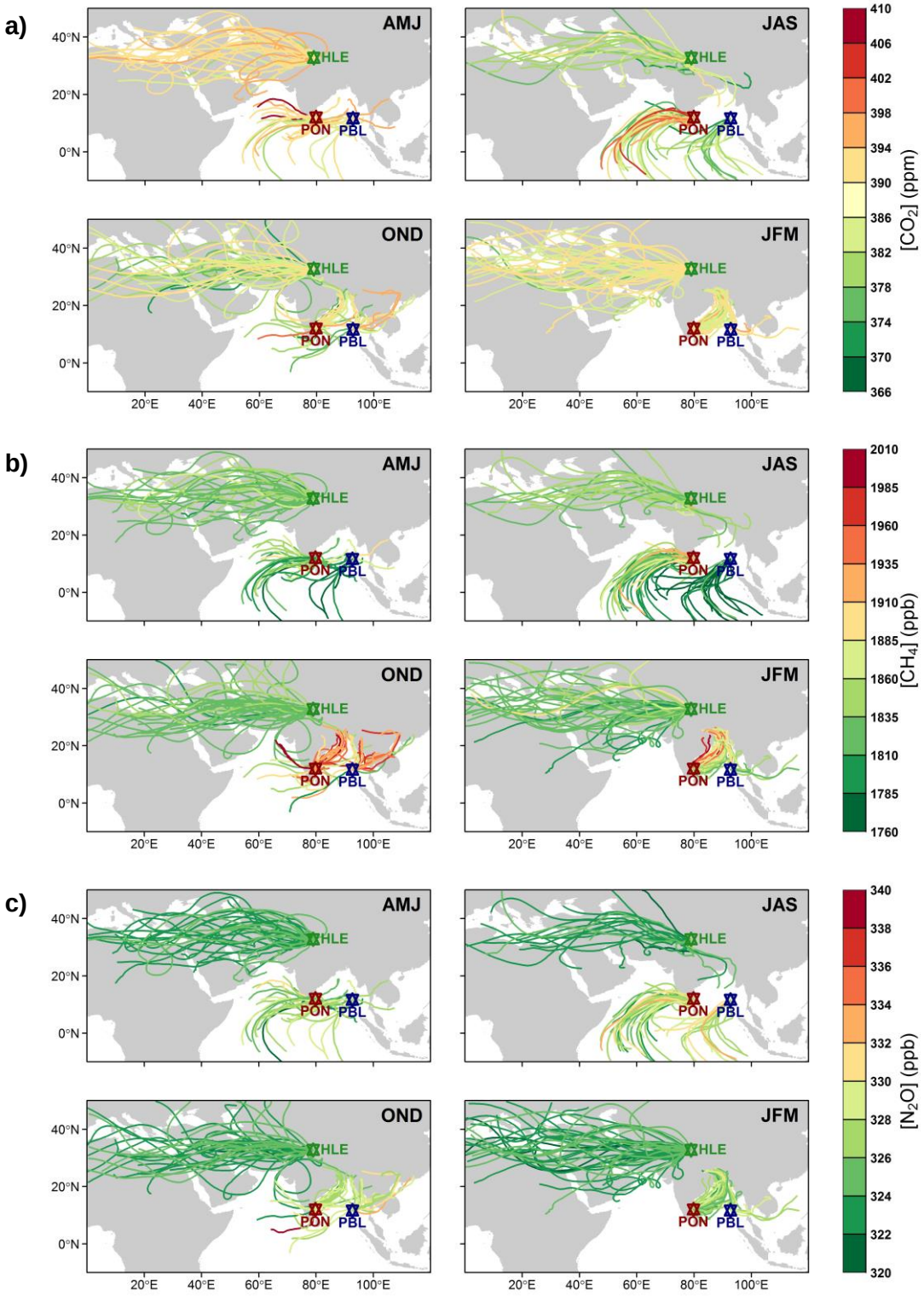

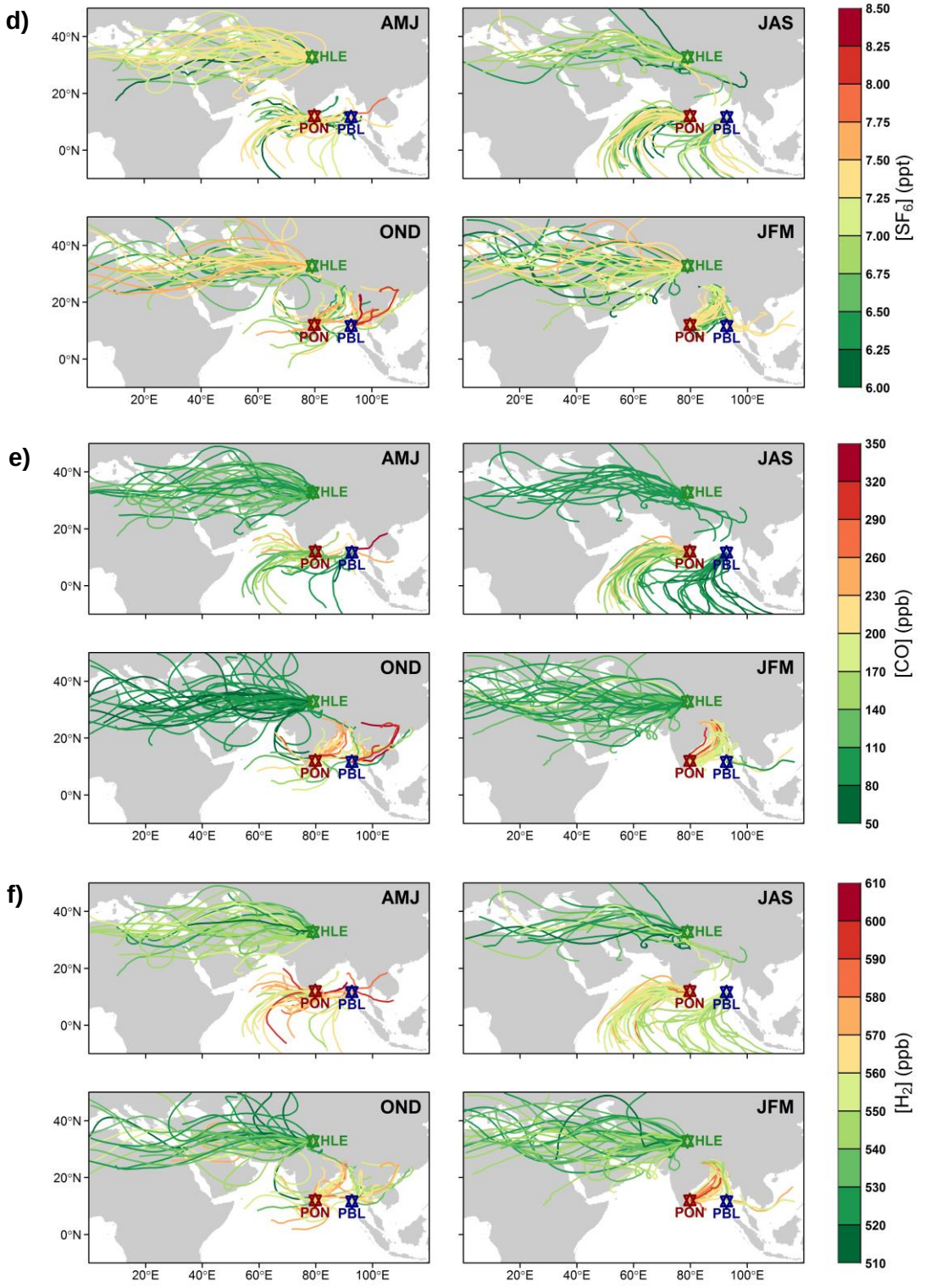
d)
AMJ
JAS
OND
JFM
HLE
PON
PBL
40°N
20°N
0°N
20°E
40°E
60°E
80°E
100°E
8.50
8.25
8.00
7.75
7.50
7.25
7.00
6.75
6.50
6.25
6.00
[SF6] (ppt)
e)
350
320
290
260
230
200
170
140
110
80
50
[CO] (ppb)
f)
610
600
590
580
570
560
550
540
530
520
510
[H2] (ppb)

Figure S8 Five-day back trajectories calculated for all sampling hours of the in situ CO_2 measurements over New Delhi by the CONTRAIL project (2006–2010). Back trajectories are computed and plotted at different altitude bands: **(a)** 3–4 km, **(b)** 4–5 km, and **(c)** 5–6 km. For comparison, back trajectories for all sampling dates of the flask measurements at HLE (2007–2011) are also presented in **(d)**. All back trajectories are colored by the elevation of air masses at hourly time step.

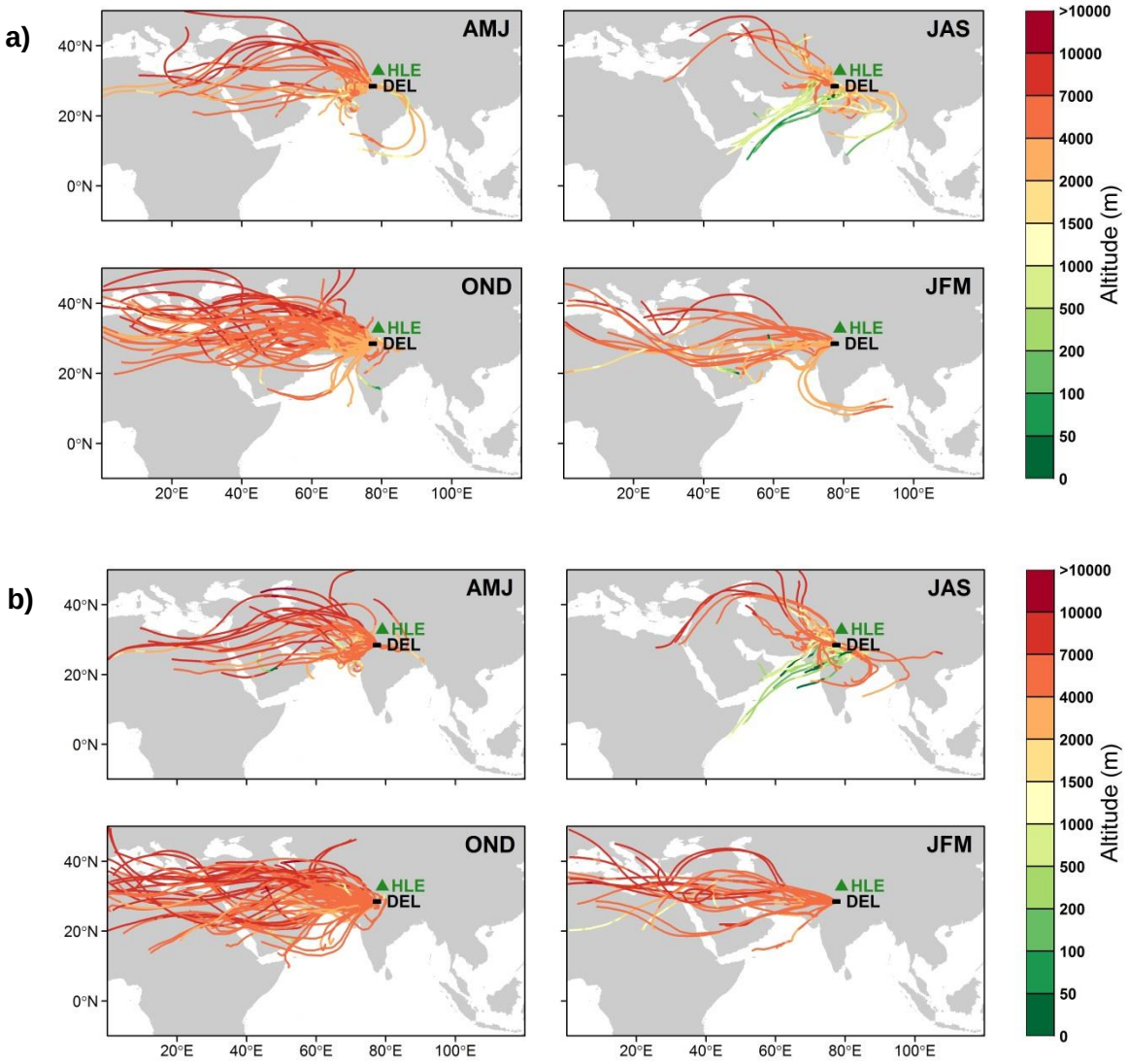

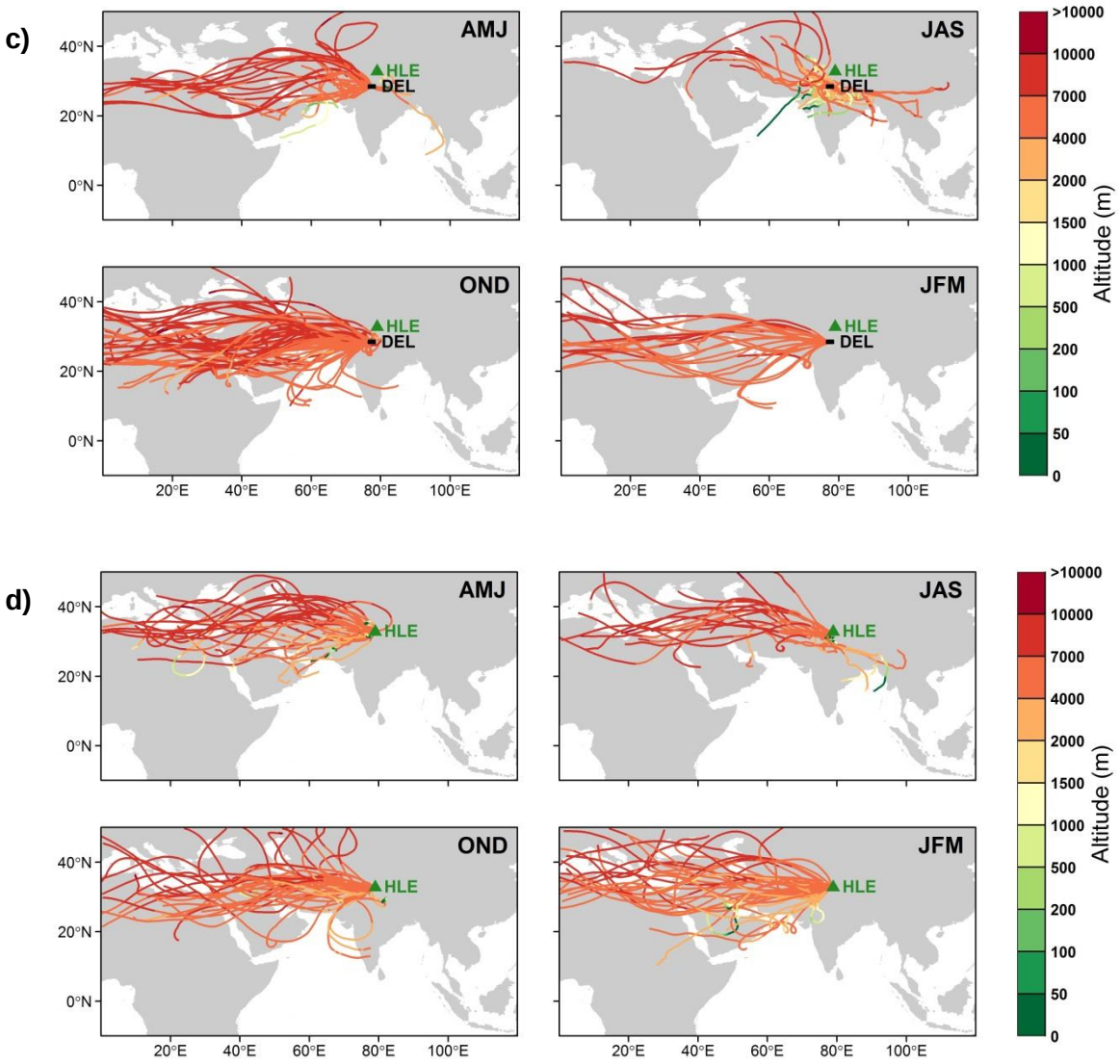
c)
AMJ
JAS
OND
JFM
HLE
DEL
40°N
20°N
0°N
20°E
40°E
60°E
80°E
100°E
>10000
10000
7000
4000
2000
1500
1000
500
200
100
50
0
Altitude (m)
d)
AMJ
JAS
OND
JFM
HLE
40°N
20°N
0°N
20°E
40°E
60°E
80°E
100°E
>10000
10000
7000
4000
2000
1500
1000
500
200
100
50
0
Altitude (m)

Figure S9 (a) Five-day back trajectories calculated for all sampling hours of the flask measurements by the CARIBIC flight between Frankfurt and Chennai at flight altitudes 8–12.5 km for the year 2008. The box indicates the domain of 10–40°N, 50–80°E, where flask samples within it were investigated in Schuck et al. (2010). **(b)** Five-day back trajectories calculated for all sampling dates over the period 2007–2011 at HLE. All back trajectories are colored by the elevation of air masses at hourly time step.

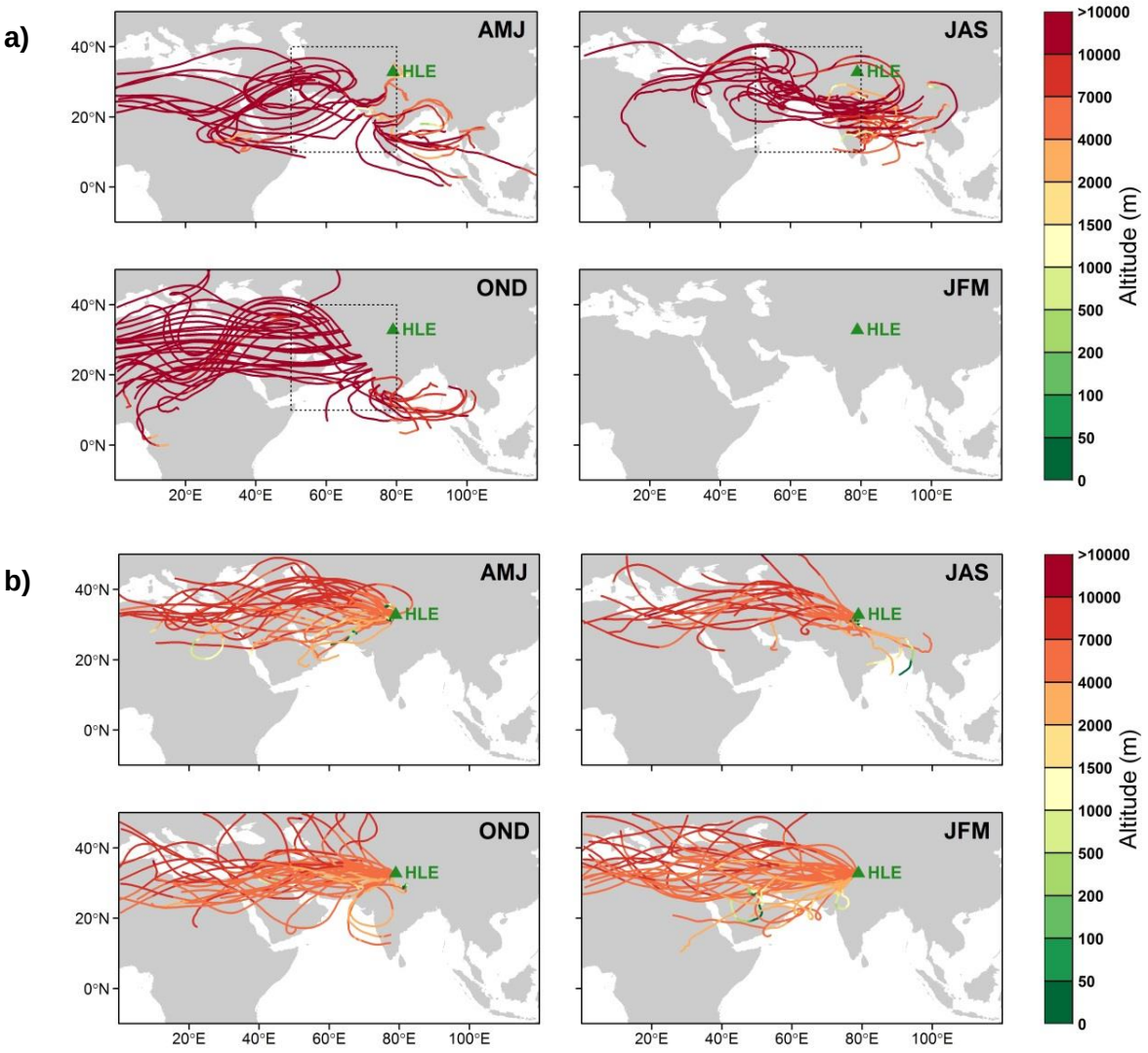

Figure S10 Time series of N_2O flask measurements at **a)** MHD, BGU, FIK and LPO, and **b)** NWR, HFM and LEF. The open circles denotes flask data used to fit the smoothed curves, while the crosses denotes discarded flask data lying outside 3 times the residual standard deviations from the smoothed curve fits. For each station, the smoothed curve is fitted using Thoning's method (Thoning et al., 1989) after removing outliers. Here HLE, MHD, BGU, FIK and LPO belong to the ICOS network, whereas NWR, HFM and LEF belong to the NOAA/ESRL network (Table S6, Figure S1).

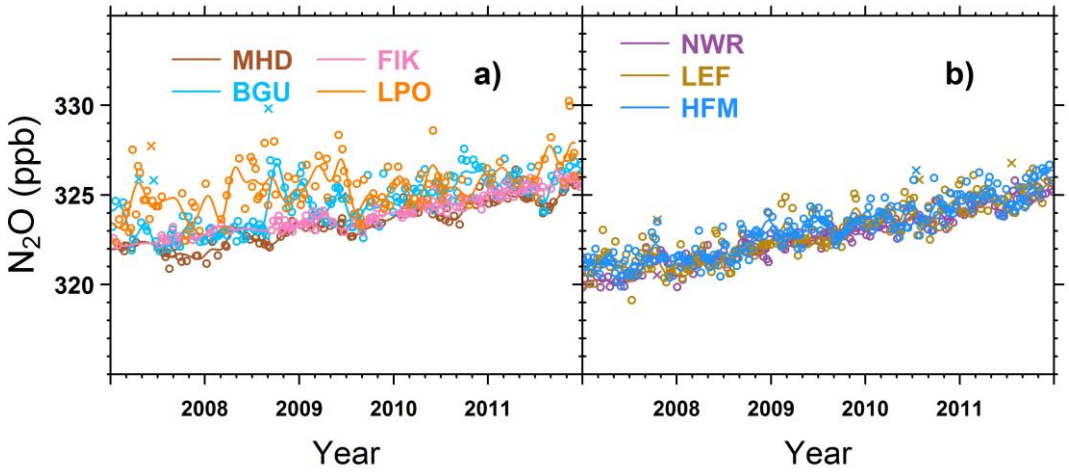

Figure S11 The mean N_2O seasonal cycles observed at HLE and MHD. For each station, the mean seasonal cycle is calculated based on the curve fitting procedures of N_2O flask data. Shaded area indicates the uncertainty of the mean seasonal cycle calculated from 1 SD of 1000 bootstrap replicates.

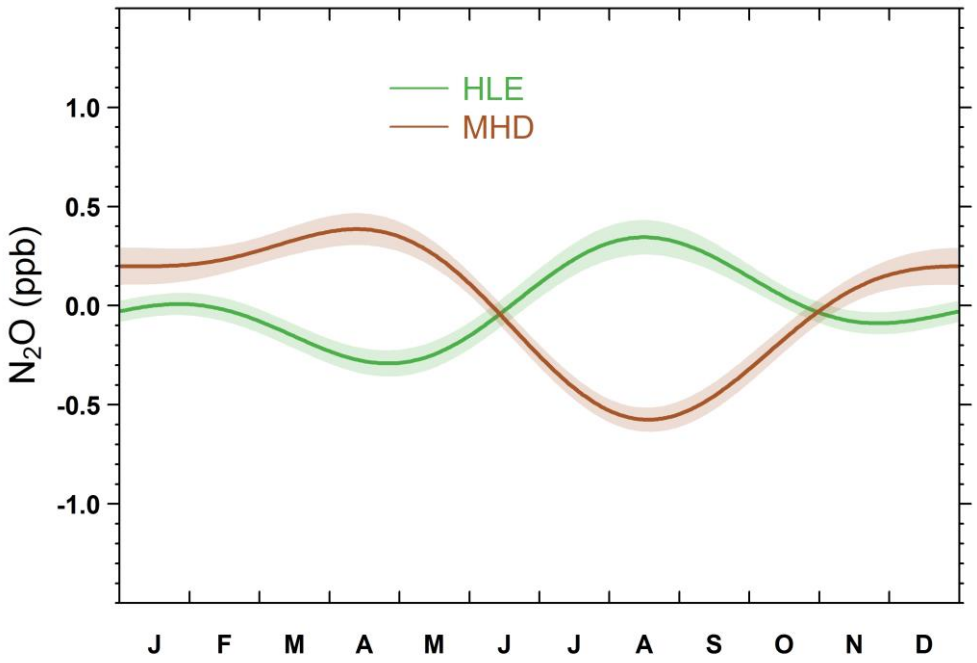

Figure S12 Time series of SF_6 flask measurements at **a)** HLE and MLO, **b)** MHD, BGU and LPO, and **c)** NWR and HFM. The open circles denote flask data used to fit the smoothed curves. For each station, the smoothed curve is fitted using Thoning's method (Thoning et al., 1989) after removing outliers. Here HLE, MHD, BGU and LPO belong to the ICOS network, whereas MLO, NWR and HFM belong to the NOAA/ESRL network (Table S6, Figure S1).

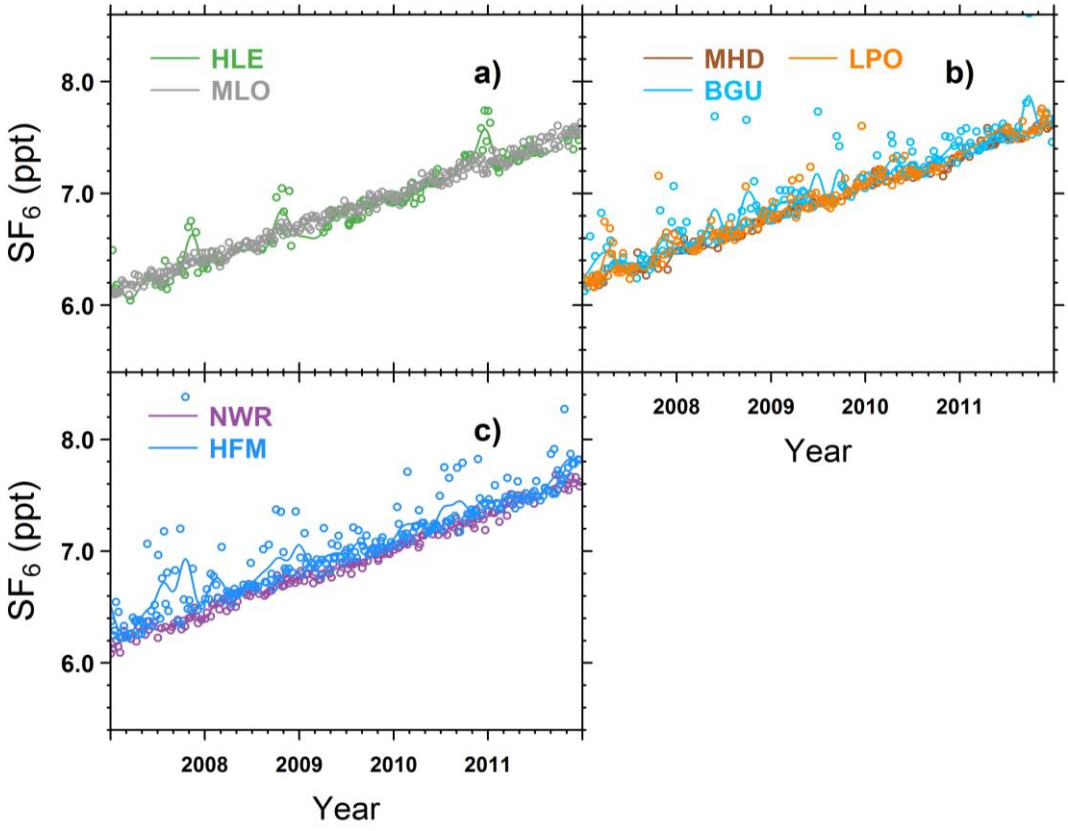

Figure S13 Time series of H_2 flask measurements at **a)** HLE and BMW, **b)** HLE and MID, **c)** PON and PBL, and **d)** PON and GMI. The open circles denote flask data used to fit the smoothed curves, while the crosses denotes discarded flask data lying outside 3 times the residual standard deviations from the smoothed curve fits. For each station, the smoothed curve is fitted using Thoning's method (Thoning et al., 1989) after removing outliers.

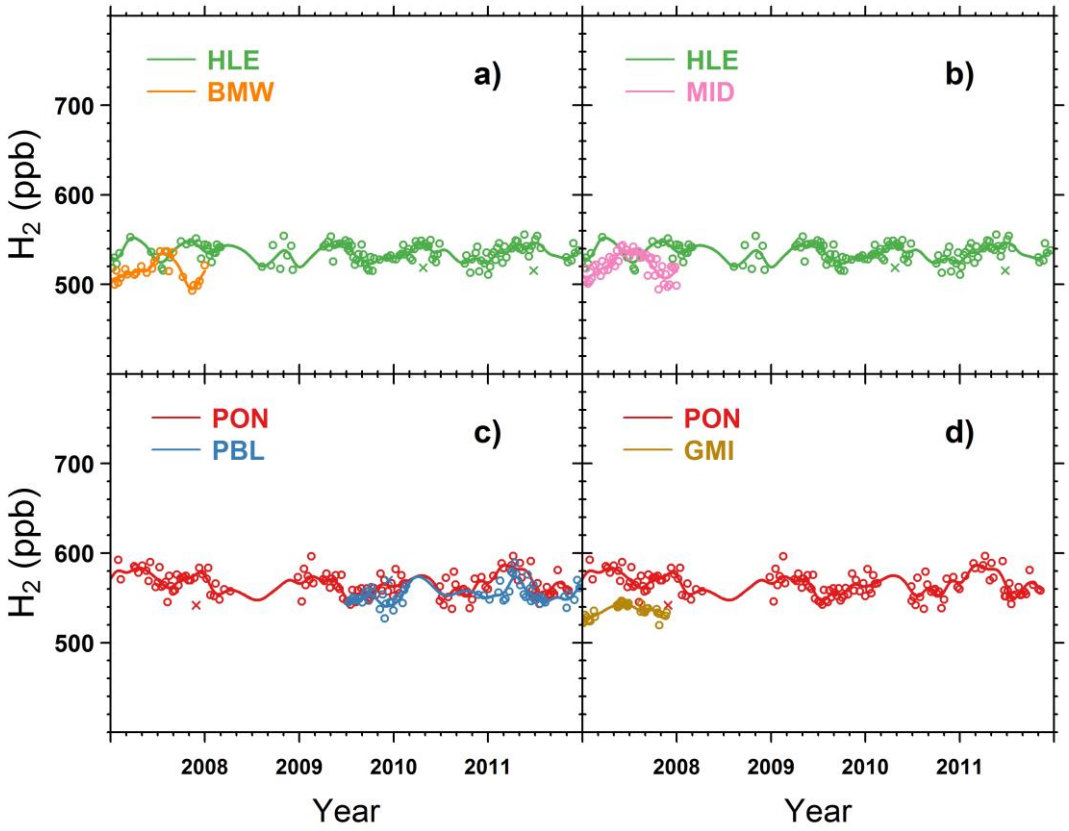

Figure S14 The mean H_2 seasonal cycles observed at **a)** HLE, BMI and MID, and **b)** PON, PBL and GMI. For each station, the mean seasonal cycle is calculated based on the curve fitting procedures of H_2 flask data. Shaded area indicates the uncertainty of the mean seasonal cycle calculated from 1 SD of 1000 bootstrap replicates.

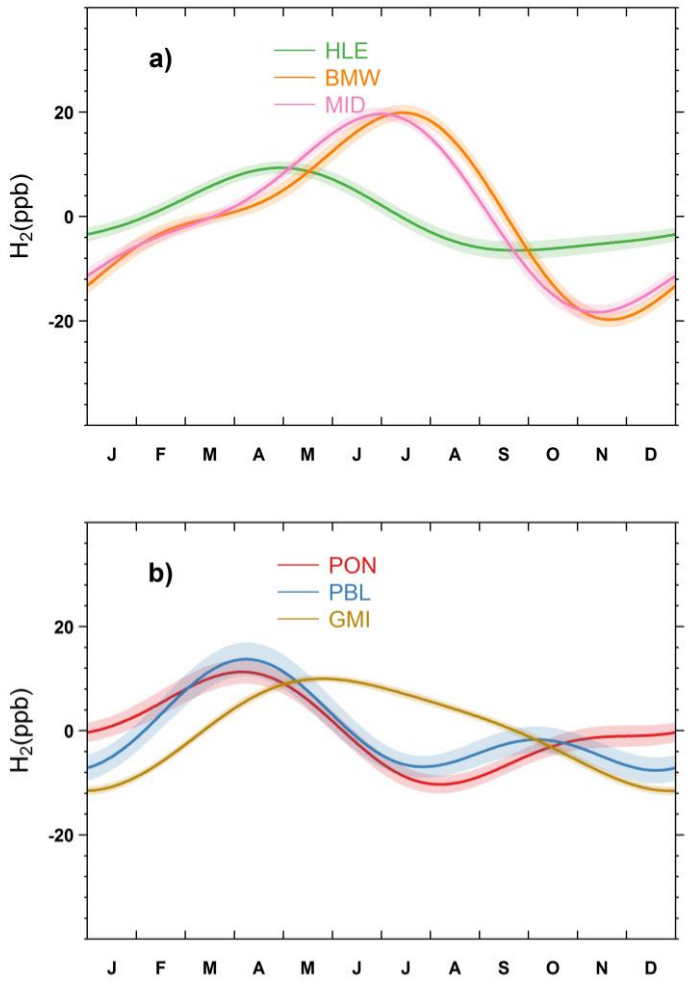

Figure S15 The CH_4/CO_2 ratio for **a)** July–September and **b)** January–March from the CARIBIC flask measurements at the altitudes of 10-12 km over India south of 20°N. Flasks were sampled during the flight from/to Chennai, India (MAA) over the period of July-September, 2008 and January–March, 2012, respectively.

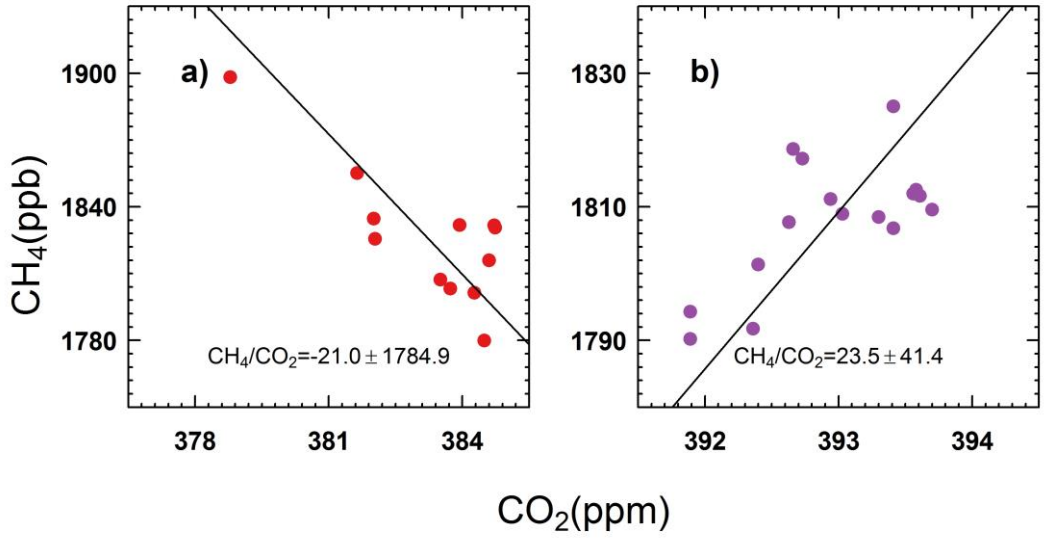

240 **Figure S16** Daily assimilated fire radiative power ($mW \cdot m^{-2}$) during **a)** Sep. 2 – Sep. 7, 2009
241 and **b)** Jul. 15–Jul. 20, 2011, corresponding to the CH_4 and CO events at BKT in Figure 17.
242 The fire radiative power data is derived from Global Fire Assimilation System (GFAS)
243 products version 1.0, with a spatial resolution of 0.5° (Kaiser et al., 2012).

244

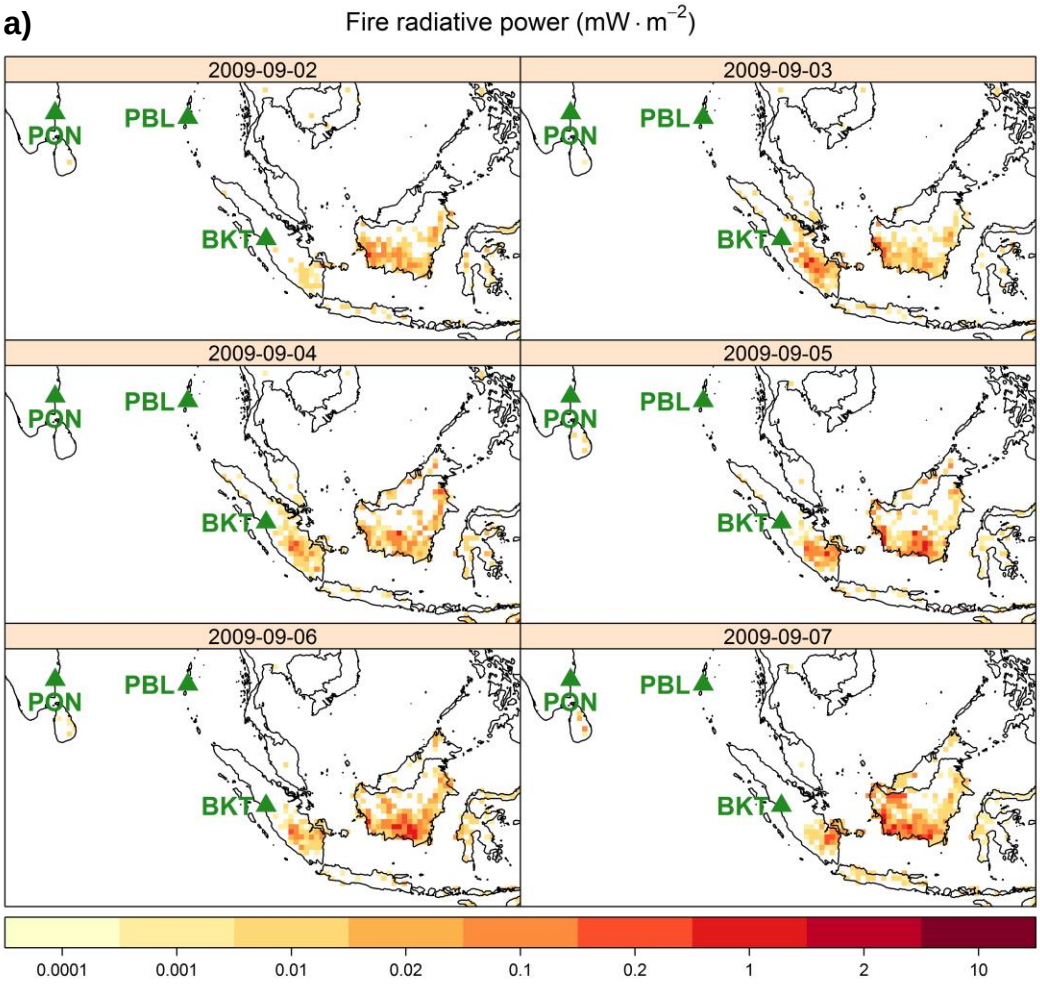

245

246

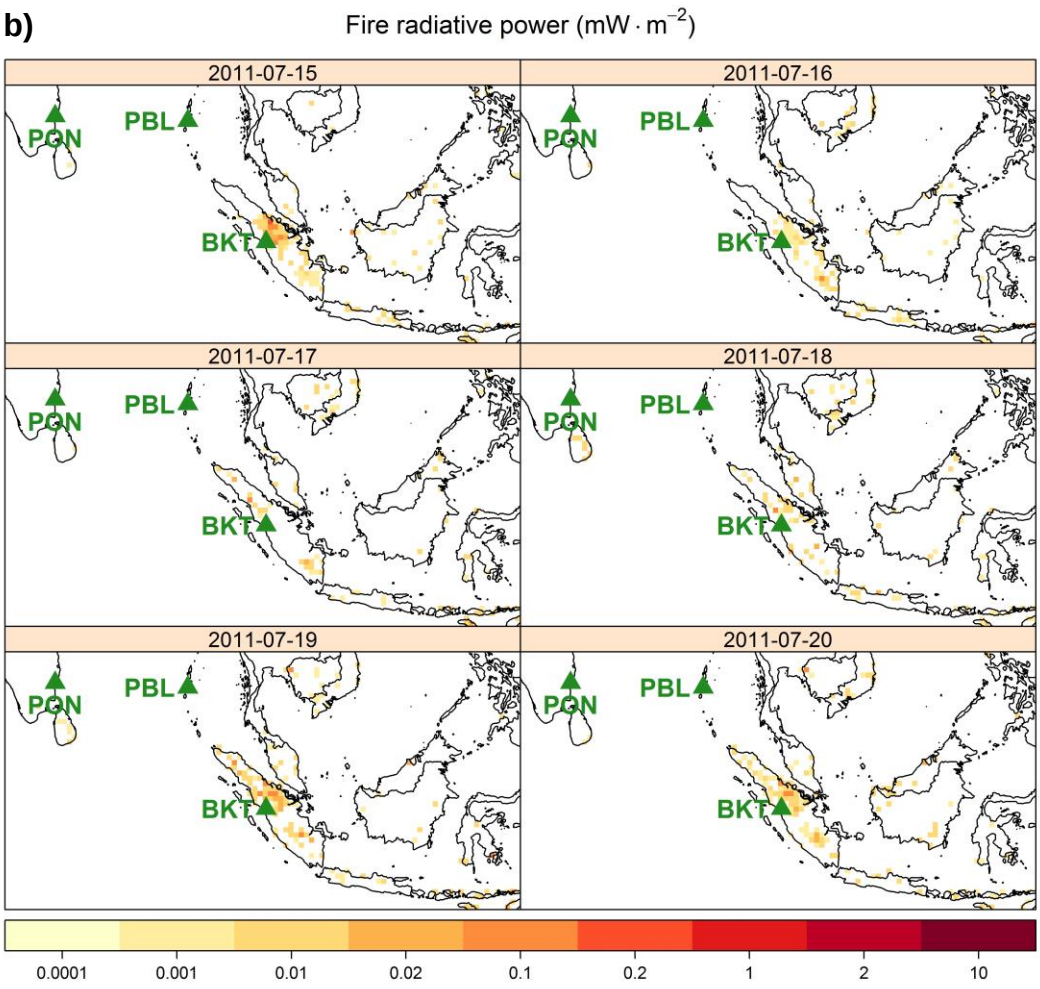
b)
Fire radiative power (mW · m^{-2})
2011-07-15
2011-07-16
2011-07-17
2011-07-18
2011-07-19
2011-07-20
PGN
PBL
BKT
0.0001
0.001
0.01
0.02
0.1
0.2
1
2
10

References

Bakwin, P. S., Tans, P. P., Zhao, C., Ussler, W., and Quesnell, E.: Measurements of carbon dioxide on a very tall tower, Tellus B, 47, 535-549, 10.1034/j.1600-0889.47.issue5.2.x, 1995.

Chi, X., Winderlich, J., Mayer, J. C., Panov, A. V., Heimann, M., Birmili, W., Heintzenberg, J., Cheng, Y., and Andreae, M. O.: Long-term measurements of aerosol and carbon monoxide at the ZOTTO tall tower to characterize polluted and pristine air in the Siberian taiga, Atmos. Chem. Phys., 13, 12271-12298, 10.5194/acp-13-12271-2013, 2013.

Harris, J. M., Dlugokencky, E. J., Oltmans, S. J., Tans, P. P., Conway, T. J., Novelli, P. C., Thoning, K. W., and Kahl, J. D. W.: An interpretation of trace gas correlations during Barrow, Alaska, winter dark periods, 1986–1997, J. Geophys. Res.: Atmos., 105, 17267-17278, 10.1029/2000jd900167, 2000.

Harriss, R. C., Sachse, G. W., Collins, J. E., Wade, L., Bartlett, K. B., Talbot, R. W., Browell, E. V., Barrie, L. A., Hill, G. F., and Burney, L. G.: Carbon monoxide and methane over Canada: July–August 1990, J. Geophys. Res.: Atmos., 99, 1659-1669, 10.1029/93jd01906, 1994.

Kaiser, J. W., Heil, A., Andreae, M. O., Benedetti, A., Chubarova, N., Jones, L., Morcrette, J. J., Razinger, M., Schultz, M. G., Suttie, M., and van der Werf, G. R.: Biomass burning emissions estimated with a global fire assimilation system based on observed fire radiative power, Biogeosciences, 9, 527-554, 10.5194/bg-9-527-2012, 2012.

Lai, S. C., Baker, A. K., Schuck, T. J., van Velthoven, P., Oram, D. E., Zahn, A., Hermann, M., Weigelt, A., Slemr, F., Brenninkmeijer, C. A. M., and Ziereis, H.: Pollution events observed during CARIBIC flights in the upper troposphere between South China and the Philippines, Atmos. Chem. Phys., 10, 1649-1660, 10.5194/acp-10-1649-2010, 2010.

Niwa, Y., Tsuboi, K., Matsueda, H., Sawa, Y., Machida, T., Nakamura, M., Kawasato, T., Saito, K., Takatsuji, S., Tsuji, K., Nishi, H., Dehara, K., Baba, Y., Kuboike, D., Iwatsubo, S., Ohmori, H., and Hanamiya, Y.: Seasonal Variations of CO_2, CH_4, N_2O and CO in the Mid-Troposphere over the Western North Pacific Observed Using a C-130H Cargo Aircraft, J. Meteor. Soc. Japan. Ser. II, 92, 55-70, 10.2151/jmsj.2014-104, 2014.

Sawa, Y., Matsueda, H., Makino, Y., Inoue, H. Y., Murayama, S., Hirota, M., Tsutsumi, Y., Zaizen, Y., Ikegami, M., and Okada, K.: Aircraft Observation of CO_2, CO, O_3 and H_2 over the North Pacific during the PACE-7 Campaign, Tellus B, 56, 2-20, 10.1111/j.1600-0889.2004.00088.x, 2004.

Wada, A., Matsueda, H., Sawa, Y., Tsuboi, K., and Okubo, S.: Seasonal variation of enhancement ratios of trace gases observed over 10 years in the western North Pacific, Atmos. Environ., 45, 2129-2137, http://dx.doi.org/10.1016/j.atmosenv.2011.01.043, 2011.

Xiao, Y., Jacob, D. J., Wang, J. S., Logan, J. A., Palmer, P. I., Suntharalingam, P., Yantosca, R. M.,Sachse, G. W., Blake, D. R., and Streets, D. G.: Constraints on Asian and European sources ofmethane from CH_4-C_2H_6-CO correlations in Asian outflow, J. Geophys. Res.: Atmos., 109, D15S16, 10.1029/2003jd004475, 2004.